

UNCLASSIFIED

READ INSTRUCTIONS BEFORE COMPLETING FORM

ADA 043898

1. REPORT NUMBER	2. GOVT ACCESSION NO.	3. RECIPIENT'S CATALOG NUMBER
4. TITLE (and Subtitle) <b>AIR-TO-WATER BLAST WAVE TRANSFER,</b>		5. TYPE OF REPORT & PERIOD COVERED
7. AUTHOR(s) Phillip J. Peckham		6. PERFORMING ORG. REPORT NUMBER
PERFORMING ORGANIZATION NAME AND ADDRESS Naval Surface Weapons Center White Oak Silver Spring, MD 20910		8. CONTRACT OR GRANT NUMBER(s)  16 17
11. CONTROLLING OFFICE NAME AND ADDRESS Strategic Systems Project Office Department of the Navy Washington, D.C. 20376		10. PROGRAM ELEMENT, PROJECT, TASK AREA & WORK UNIT NUMBERS 64363N; B0003; B0003001 WR 14DA
14. MONITORING AGENCY NAME & ADDRESS (if different from Controlling Office)  12 22 p.		12. REPORT DATE 11 1976
		13. NUMBER OF PAGES 20
		15. SECURITY CLASS. (of this report)  UNCLASSIFIED
		15a. DECLASSIFICATION/DOWNGRADING SCHEDULE
16. DISTRIBUTION STATEMENT (of this Report)  Approved for public release; distribution unlimited.		
17. DISTRIBUTION STATEMENT (of the abstract entered in Block 20, if different from Report)		
18. SUPPLEMENTARY NOTES		
<p>DDC FILE COPY</p> <p>KEY WORDS (Continue on reverse side if necessary and identify by block number)</p> <p>Shock waves Explosive shock waves Underwater shock waves Airblast shock waves. Explosives</p> <p>ABSTRACT (Continue on reverse side if necessary and identify by block number)</p> <p>A study to characterize the shock wave induced in the water directly below an explosion in air has been carried out. Spherical and cylindrical charges weighing up to 3.63 kilograms were fired. Burst heights extended from 1.58 meters/kilogram <sup>1/3</sup> down to the water/air interface. All cylinders were fired with their major axis perpendicular to the water surface. Both the airblast and underwater shock waves were measured.</p> <p>Both the spherical and cylindrical charges produced underwater pressure-time histories that were characterized by multiple pressure pulses. Those from cylinders were more reproducible.</p>		

DDC  
RECORDED  
SEP 9 1977  
A

1 JAN 73 1473

EDITION OF 1 NOV 65 IS OBSOLETE  
S/N 0102-014-6601

391 596 UNCLASSIFIED

AIR-TO-WATER BLAST WAVE TRANSFER

A study to characterize the shock wave induced in the water directly below an explosion in air has been carried out. Spherical and cylindrical charges weighing up to 3.63 kilograms were fired. Burst heights extended from 1.58 meters/kilogram<sup>1/3</sup> down to the water/air interface.. All cylinders were fired with their major axis perpendicular to the water surface. Both the airblast and underwater shock waves were measured.

Both the spherical and cylindrical charges produced underwater pressure-time histories that were characterized by multiple pressure pulses. Those from cylinders were more reproducible. High speed photography indicated that the major contribution to the underwater shock wave from cylinders came from the explosion products and their bow shock off the end of the cylinder. Contributions to the underwater shock from both spheres and cylinders were confined to the small area at the water/air interface directly beneath the charge. The underwater shock waves from cylinders appeared to have been produced by a smaller, more intense source than did those from spheres. Thus, the underwater pressures from cylinders decayed more rapidly with distance than did those from spheres.

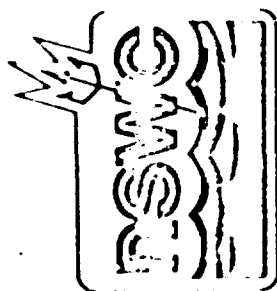
APPROPRIATE FOR	
PHYS	White Section <input checked="" type="checkbox"/>
...	Dark Section <input type="checkbox"/>
...	...
BY	...

A

Enclosure (1)

76-222

PHOTODUPLICATION CENTER



**AIR-TO-WATER  
BLAST WAVE TRANSFER**

by

**P. J. Peckham**

**Naval Surface Weapons Center**

## AIR-TO-WATER BLAST WAVE TRANSFER

### 1. Introduction

Data on the underwater blast waves transmitted across an air-water interface from an explosion in air are limited. Some inconclusive data were generated at the NSWC/WOL in 1962 (References 1 and 2). In addition, data are available from a program in which 12-kg TNT spheres were fired above a water surface and underwater pressures were measured (reference 3). To add to this paucity of data, the NSWC/WOL is conducting a program to study the effects of airblast induced underwater shocks from both cylindrical and spherical charges.

The data discussed here came from pentolite spheres and cylinders weighing either 0.454 or 3.63 kg. The spherical charge data are from centrally initiated spheres fired at scaled burst heights of 0.4 and 1.6  $\text{m/kg}^{1/3}$ . The cylindrical charge data are from cylinders with a length to diameter ratio of 3.68:1. All cylinders were fired with their major axis normal to the water surface. The point of detonation was on the major axis either at the center of the charge or one quarter of the charge length from the end of the charge toward the water. Scaled burst heights for the cylinders were either 0.4, 1.0, or 1.6  $\text{m/kg}^{1/3}$ . Data from this investigation will be available in an NSWC/WOL technical report now in the process of publication. Only the data from the cylindrical charges that were centrally detonated are discussed here.

The program was fired in an artificial pond at the NSWC/WOL test facility at Stump Neck, MD. The underwater gage array is shown in Figure 1.1. Airblast gages were flush mounted at the water surface. Seven gage positions were used extending from a point almost directly under the charge out to about 3 meters. Gages were approximately 0.4  $\text{m/kg}^{1/3}$  apart.

### 2. Comparison of the Airblast Observations

Figure 2.1 shows the airblast overpressures from pentolite spheres plotted as a function of distance along the water surface from a point beneath the charge. Curves for two scaled burst heights are shown; one at 0.4  $\text{m/kg}^{1/3}$  and the other at 1.6  $\text{m/kg}^{1/3}$ . Note that for either burst height the pressures decay smoothly from a maximum at the point most nearly beneath the charge out to the maximum measured range. Beyond a range of 1.5  $\text{m/kg}^{1/3}$ , the data converge into a single curve.

- (1) Swift, E., "Underwater Shockwaves from Explosions in Air," private communication, 4 April 1962.
- (2) Conway, M., "Investigation of the Characteristics of Air-to-Water Shocks," private communication, 11 June 1962.
- (3) Sakurai, A., and Pinkston, J., "Water Shockwaves Resulting from Explosions Above and Air-Water Interface," Waterways Experiments Station Report No. 1-771, April 1967.

The airblast overpressures from centrally detonated pentolite cylinders are shown in Figure 2.2. These are also plotted as a function of distance along the water surface from a point directly beneath the charge. Recall, the cylinders were oriented with their axis perpendicular to the water surface. Note that the airblast pressures for the two larger burst heights show a marked decrease at a range of about  $0.7 \text{ m/kg}^{1/3}$ . The pressures from the lowest burst height show no such decrease; nor does the spherical charge data in Figure 2.1.

The dips in the pressure-horizontal range curves for the two higher bursts in Figure 2.2 result from the non-spherical airblast wave front produced by a cylindrical charge explosion. Figure 2.3 shows the fireball silhouette from cylinders at the time that the fireball end lobe has just contacted the water surface. Also shown is the airblast wave front for the lower portion of the cylinder at this time. The fireball outline is traced from a high speed camera frame exposed at the time shown. The airblast wave-form is based on shadowgraph photos of the shock from a 13-gram cylinder fired under similar scaled conditions. These pictures lead to the following description of the airblast shockwave formation by a cylindrical explosion. The explosion products show strong outward motion from the ends of the cylinder along the major or long axis. In addition, outward radial motion off the sides of the cylinder takes the form of a toroid. The explosion product motion along the axis of the cylinder (or end lobe fireball growth) push a bow shock that pictures show to be attached to the explosion products at the bottom. At the same time, the radial expansion of the explosion products generate an airblast shockfront with the general toroidal shape of the explosion products. Where these two shocks would intersect a bridge wave is formed.

Airblast pressures along the water surface show the effects of the above phenomena. The reflected airblast pressures are very intense beneath the charge where the end lobe bow shock undergoes nearly normal reflection. However, as the shock propagates outward, the pressure decreases rapidly because the motion is now parallel to the water surface. (The bow shock shows no evidence of the mach stem formation associated with spherical blast wave reflection.) This rapid decay obtains until the bridge wave and the toroidal shock arrive at the water surface. Their arrival briefly increases the airblast pressures at the water surface, after which, normal pressure-distance decay begins.

The airblast pressures at the water surface from the charge fired at an HOB of 0.61 meters shows no such behavior. The bow shock arrival at the water surface is followed almost immediately by the arrival of the bridge wave and toroidal shock. Their shape in the early phase of development is almost spherical as may be seen in Figure 2.3

### 3. Underwater Blast Field

Underwater blast gages were positioned as shown in Figure 1.1. Note that the gages are positioned in 5 columns. Each column contains three gages, one gage each at scaled depths of 0.4, 0.8, and 1.6  $\text{m/kg}^{1/3}$  below the water surface. The horizontal separation between the columns was 0.8  $\text{m/kg}^{1/3}$ . Underwater blast pressure-time histories were recorded from each gage using cathode ray oscilloscopes. These records were digitized and processed on a computer to give pressure, impulse, and energy flux density in the shockwave as a function of time. In this paper, only the shockwave pressure data will be discussed.

The underwater blast field is generated by the reflection of the airblast wave front at the air-water interface. At the lower burst heights the explosion products probably contribute energy to the underwater blast. The surface area over which the airburst makes its contributions to the underwater blast field is generally very small for a spherical explosion and even smaller for a cylindrical explosion. For the spherical burst, the above area is that where regular reflection occurs. For a cylindrical explosion, the area is limited to that where the end lobe shockwave and explosion products strike the water, although the toroidal shock (Figure 2.1) makes a small contribution at positions well away from Surface Zero.

The underwater shock wave pressure-time histories induced by an airburst are similar to those from a shallow underwater explosion with two exceptions. First, they are made up of multiple pressure pulses. (See Figure 3.1) These multiple pulses result in part from the perturbations on the airblast shockfront and the explosion products front. These perturbations reflecting off the interface act as separate sources for the underwater shockwave. Thus, the underwater pressure-time history shows a number of pressure peaks corresponding to the arrival of the shock-generated by each perturbation. However, the above explanation may not account for all the spikes on the pressure-time histories. Hydrocode calculations show the possibility of a reverberation of the airshock between the product front and the water surface.

Underwater pressure-time histories recorded from a cylindrical air burst are shown in Figure 3.2. The pulse from the toroidal shock is seen in the pressure trace taken farthest from Surface Zero for the burst height of 1.6  $\text{m/kg}^{1/3}$ .

Figures 3.3 through 3.7 compare the airblast pressures measured at the air-water interface with those measured underwater at a depth of 0.4  $\text{m/kg}^{1/3}$ . Figures 3.3 and 3.4 are for spherical charges fired at burst heights of 0.4 and 1.6  $\text{m/kg}^{1/3}$ , respectively. The underwater pressures directly below the charge are down by a factor of two from the airblast pressure measured at the surface. However, as horizontal range increases, the underwater pressures rise

above the measured airblast pressures for the  $0.4 \text{ m/kg}^{1/3}$  burst height (Figure 3.3). The underwater pressures for the burst height of  $1.6 \text{ m/kg}^{1/3}$  in Figure 3.4, remain below the measured airblast pressures.

Figure 3.5 compares the airblast measured at the surface with the pressures measured underwater from a cylindrical charge burst at a height of  $0.4 \text{ m/kg}^{1/3}$ . Here, the underwater pressures follow somewhat closely, the measured airblast. Figure 3.6 compares airblast and underwater pressures from a cylinder burst at a height of  $1.6 \text{ m/kg}^{1/3}$ . In this case, there is reasonable agreement between the underwater and airblast pressures for a cylindrical burst at a height of  $1.6 \text{ m/kg}^{1/3}$  (Figure 3.7).

The above behavior fits no simple model for underwater shock-wave generation by an airburst. However, computer models are being developed and a model will be reported at a later date.

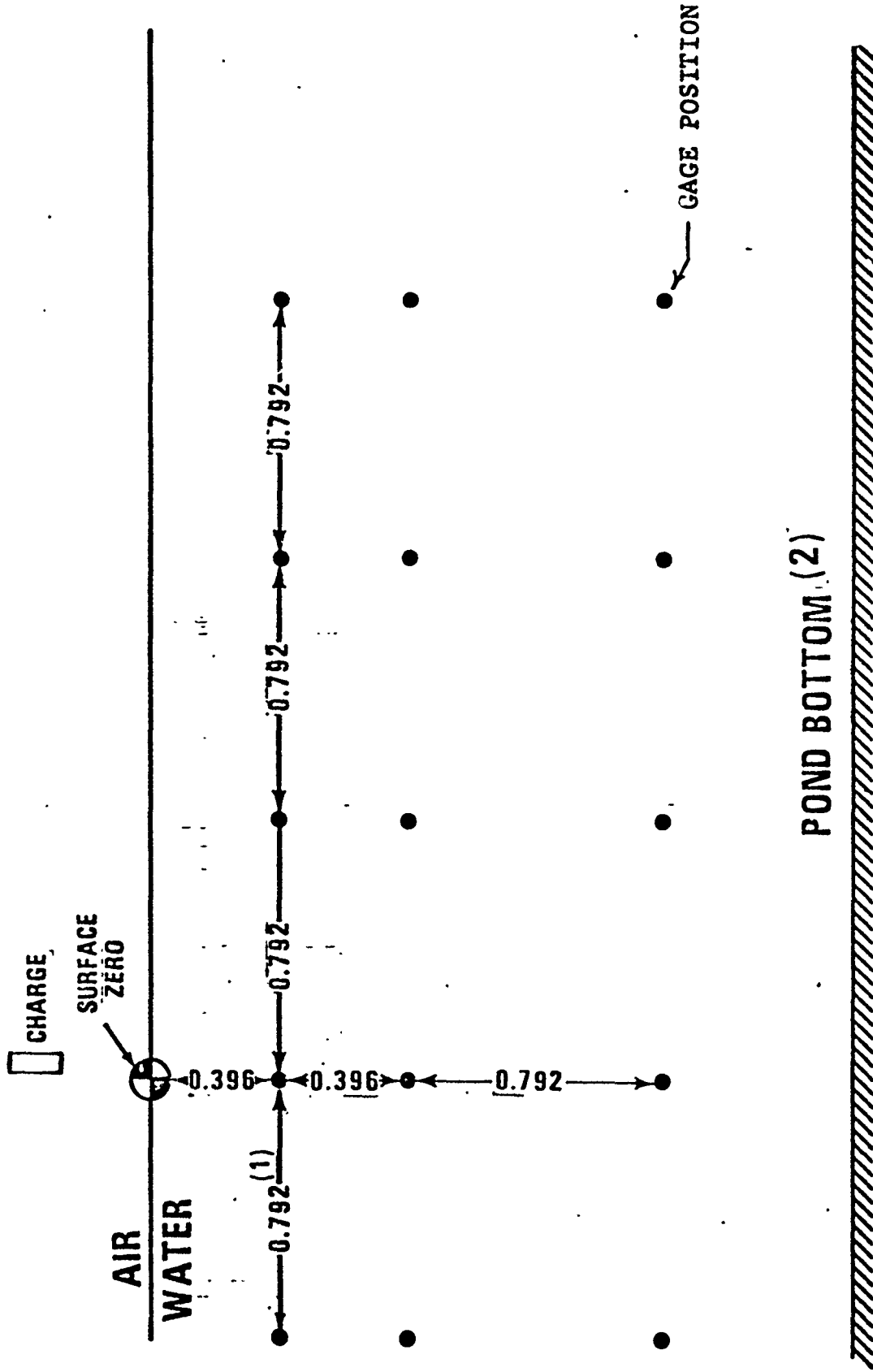
Finally, all the underwater blast pressure data obtained to date are summarized in Figures 3.8 through 3.11. These data are plotted as isopressure contours.

#### 4. Summary

Some preliminary results from a program to measure the underwater blast field produced by an explosion in air have been presented. There are differences between the blast field from cylinders and spheres but they cannot be generalized. For a burst height of  $0.4 \text{ m/kg}^{1/3}$ , the underwater blast fields are similar for cylinder and spheres. For the higher burst heights, the cylinders seem to generate a blast field giving the appearance of having come from a smaller more intense source than does the field from a spherical explosion.

# UNDERWATER GAGE ARRAY FOR POND PROGRAM

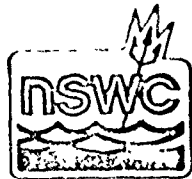
FIGURE 1.1



(1) DISTANCES ARE IN METERS/KILOGRAMS 1/3

(2) POND BOTTOM 0.46 METERS FROM LOWEST GAGE ON 3.63-KG CHARGE ARRAY  
POND BOTTOM 1.68 METERS FROM LOWEST GAGE ON 0.45-KG CHARGE ARRAY

FIGURE 2.1



# AIRBLAST PRESSURE FROM PENTOLITE SPHERES

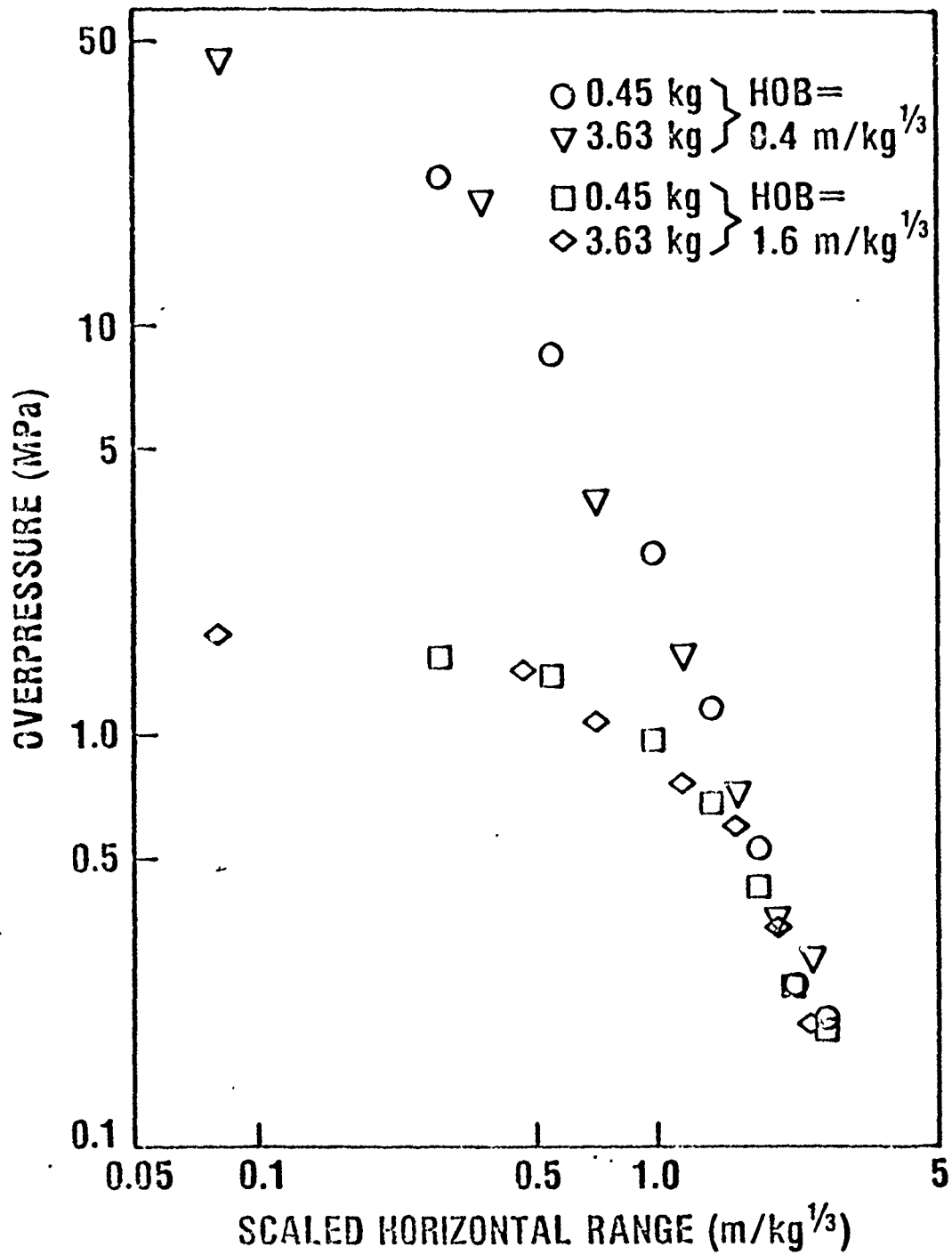
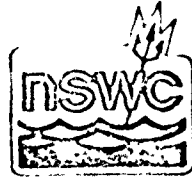
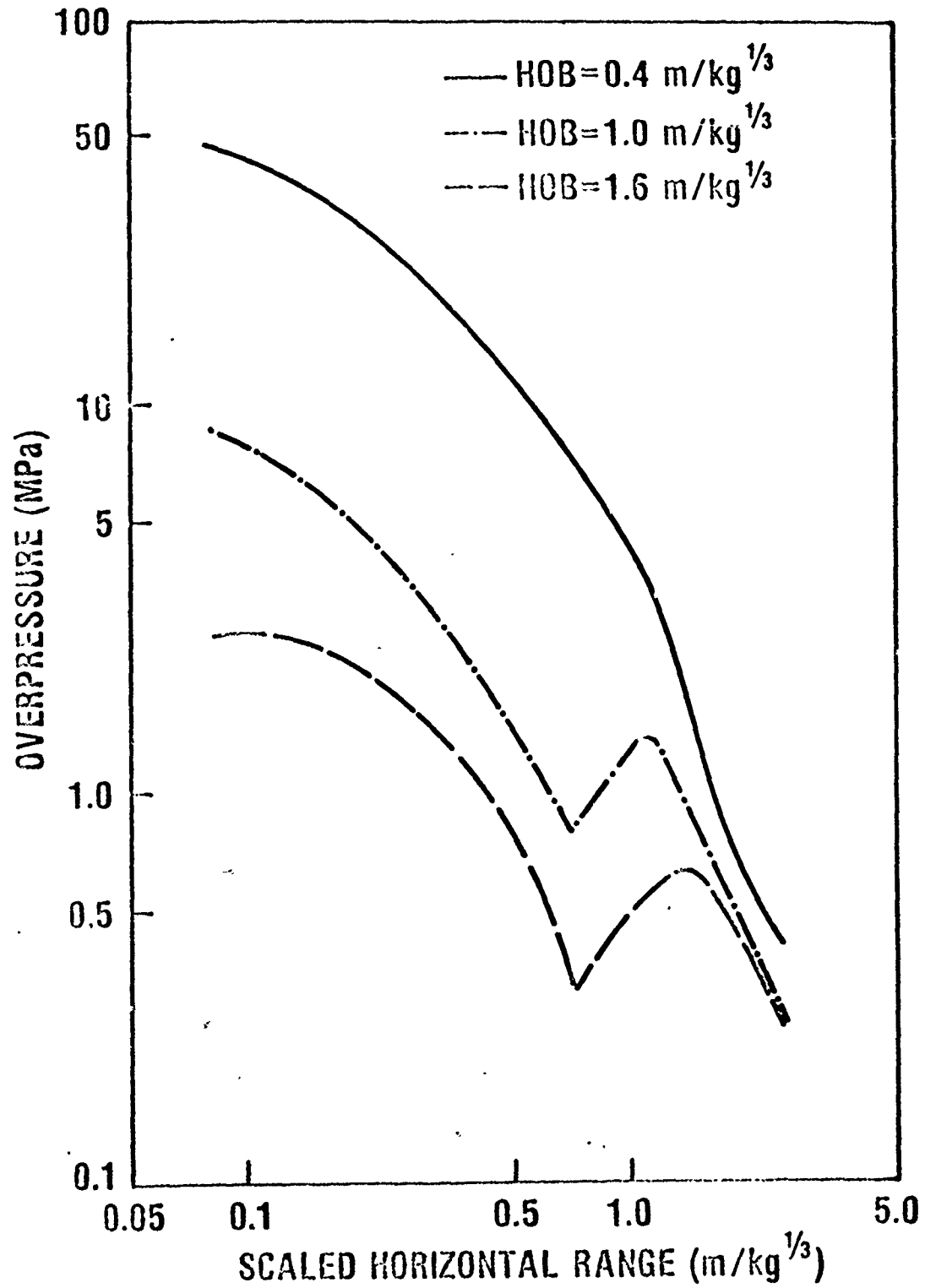
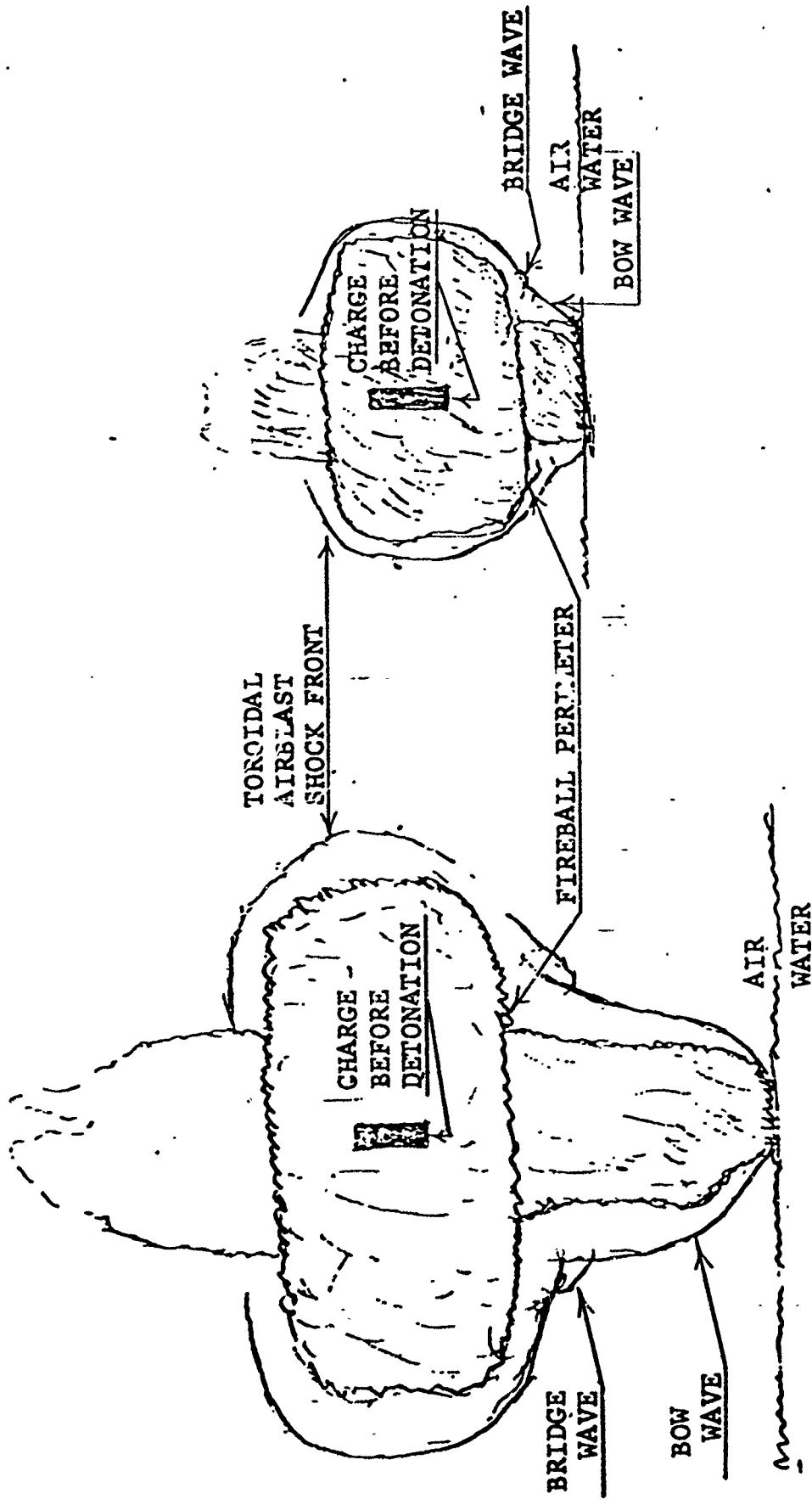


FIGURE 2.2



# AIRBLAST PRESSURES FROM PENTOLITE CYLINDERS





ABOVE DRAWING FOR 3.63 kg CYLINDER  
 FIRED 1.5 m ABOVE SURFACE; TIME  
 AFTER DETONATION = 360 us

ABOVE DRAWING FOR 3.63 kg CYLINDER  
 FIRED 0.61 m ABOVE SURFACE; TIME  
 AFTER DETONATION = 100 us

FIGURE 2.3 FIREBALL-SHOCKWAVE RELATION FOR CYLINDRICAL CHARGE  
 FIRED IN AIR NEAR A WATER SURFACE

FIGURE 3.1



# PRESSURE TIME HISTORIES FOR PENTOLITE SPHERES

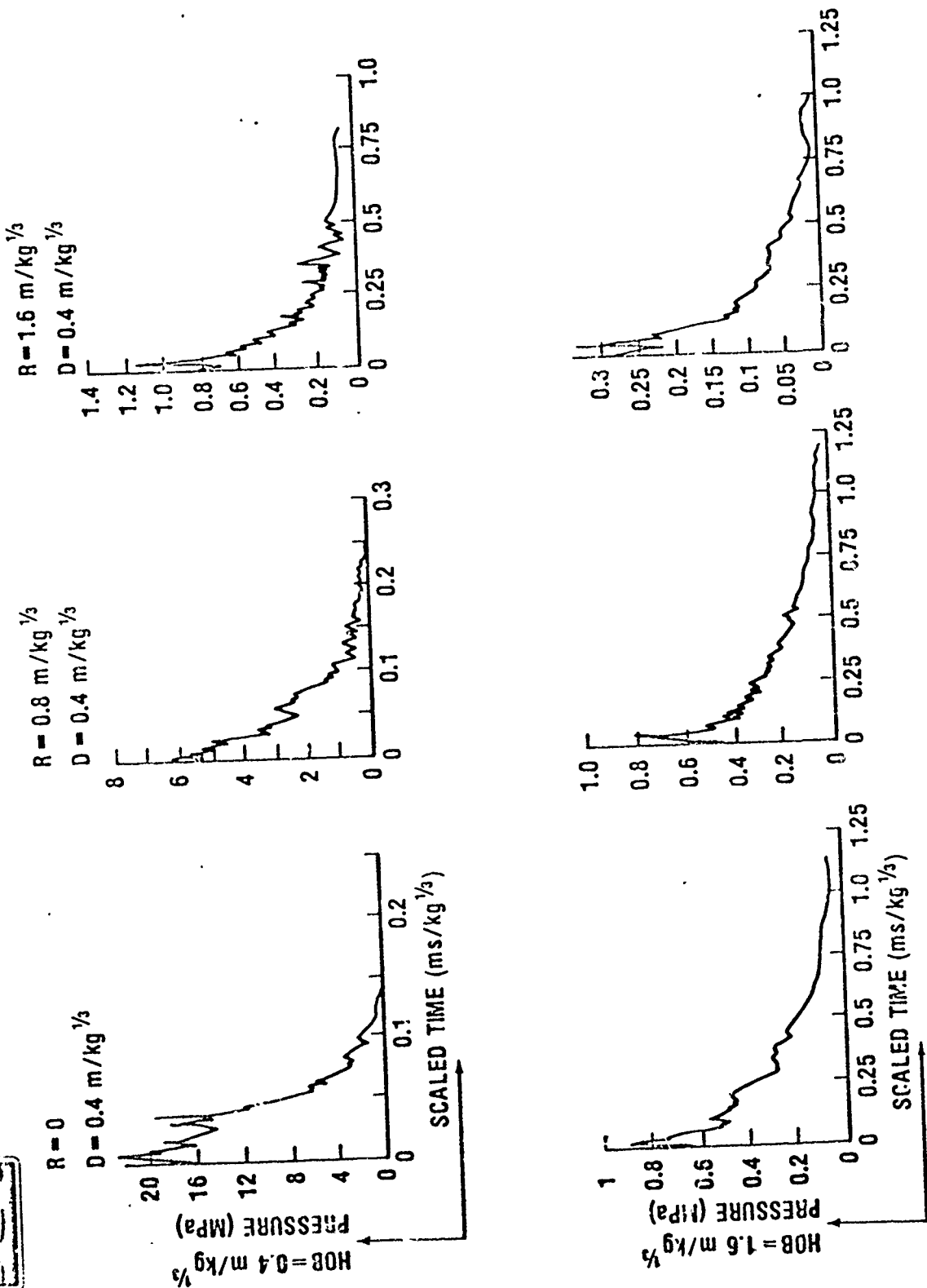




FIGURE 3.3



COMPARISON OF AIRBLAST AND UNDERWATER PRESSURES; PENTOLITE SPHERES FIRED AT  $HOB=0.4 \text{ m/kg}^{1/3}$

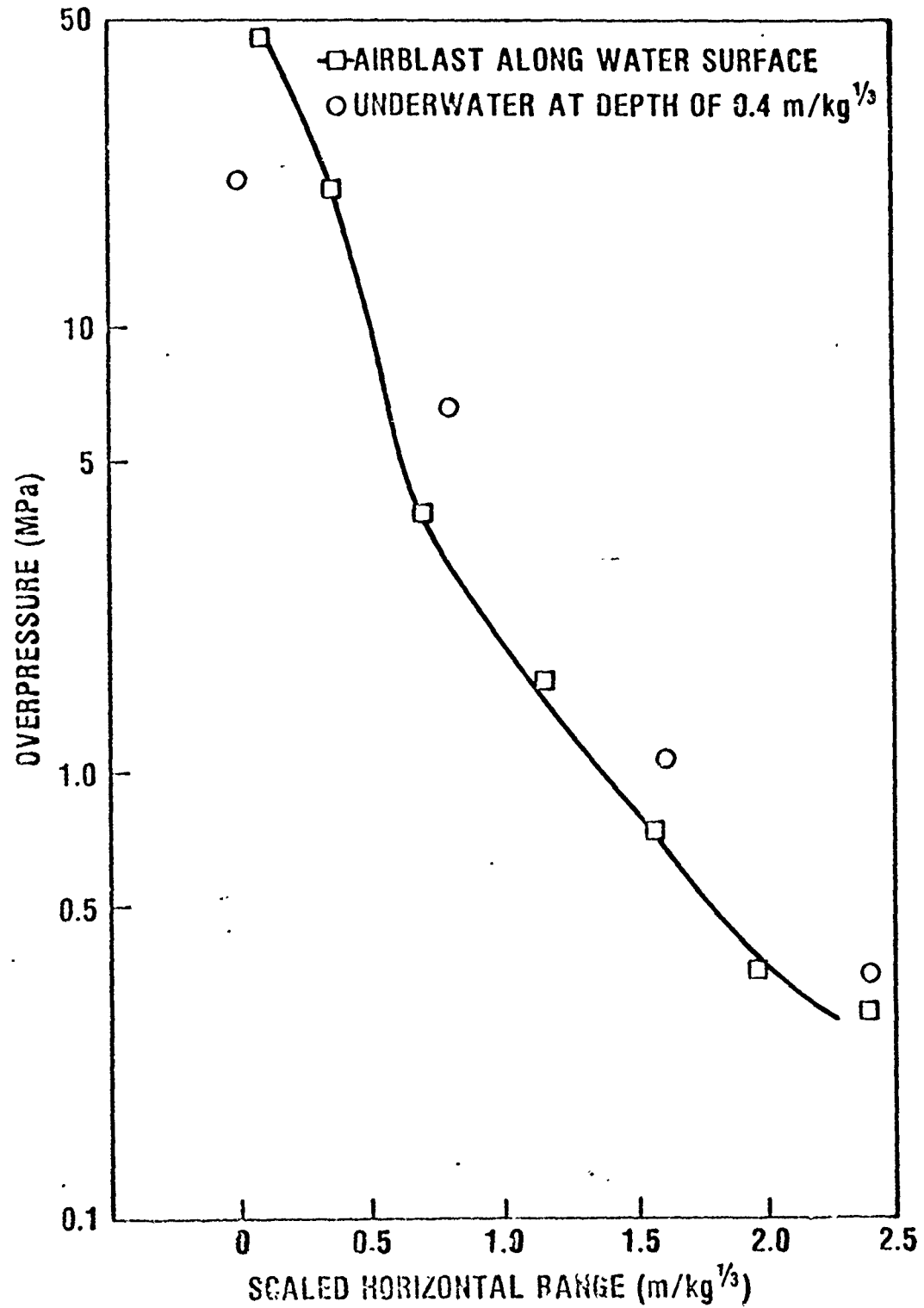


FIGURE 3.4



COMPARISON OF AIRBLAST AND UNDERWATER PRESSURES; PENTOLITE SPHERES FIRED AT  
HOB =  $1.6 \text{ m/kg}^{1/3}$

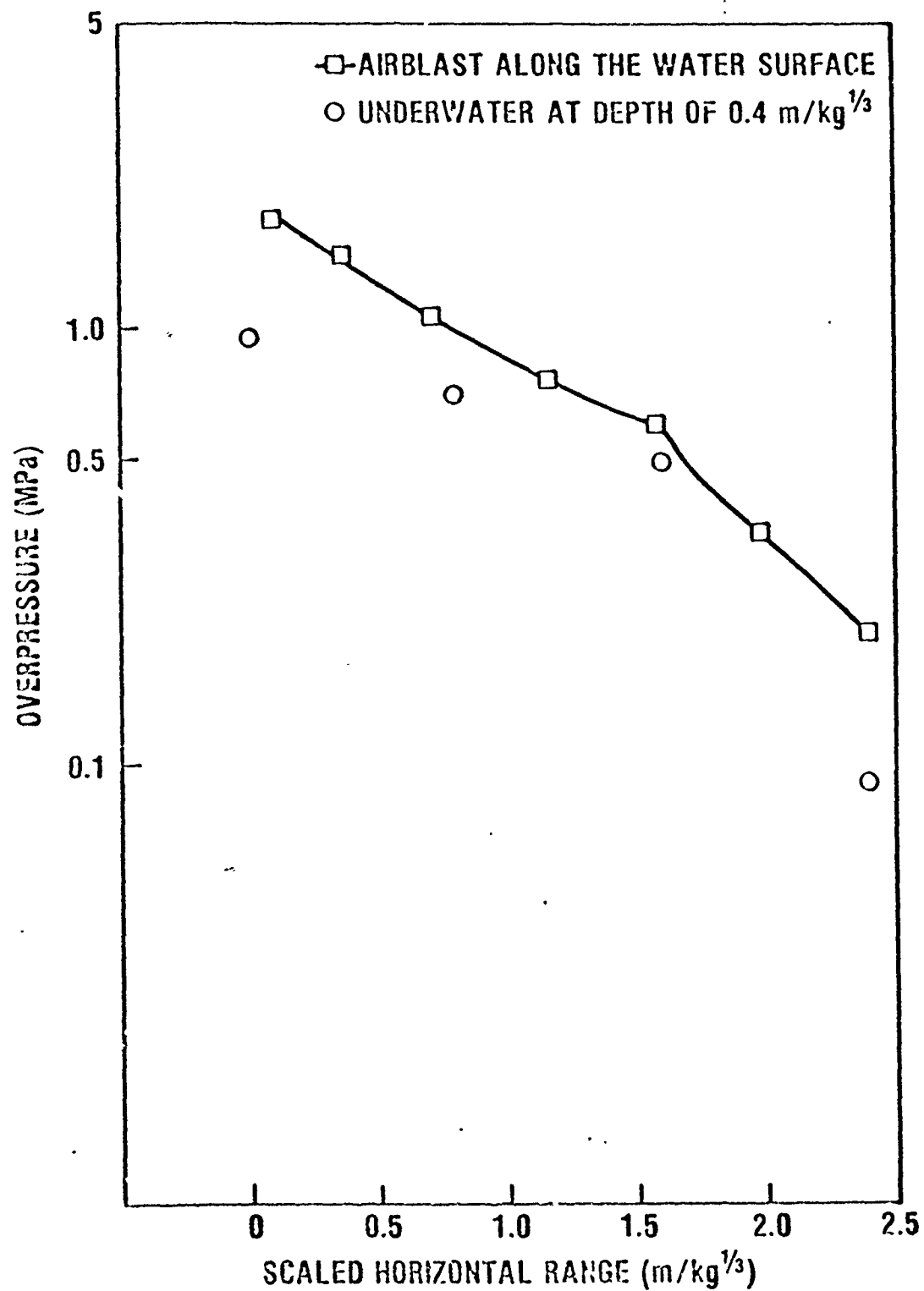


FIGURE 3.5



COMPARISON OF AIRBLAST AND UNDERWATER PRESSURES; PENTOLITE CYLINDERS FIRED AT HOB=0.4 m/kg<sup>1/3</sup>

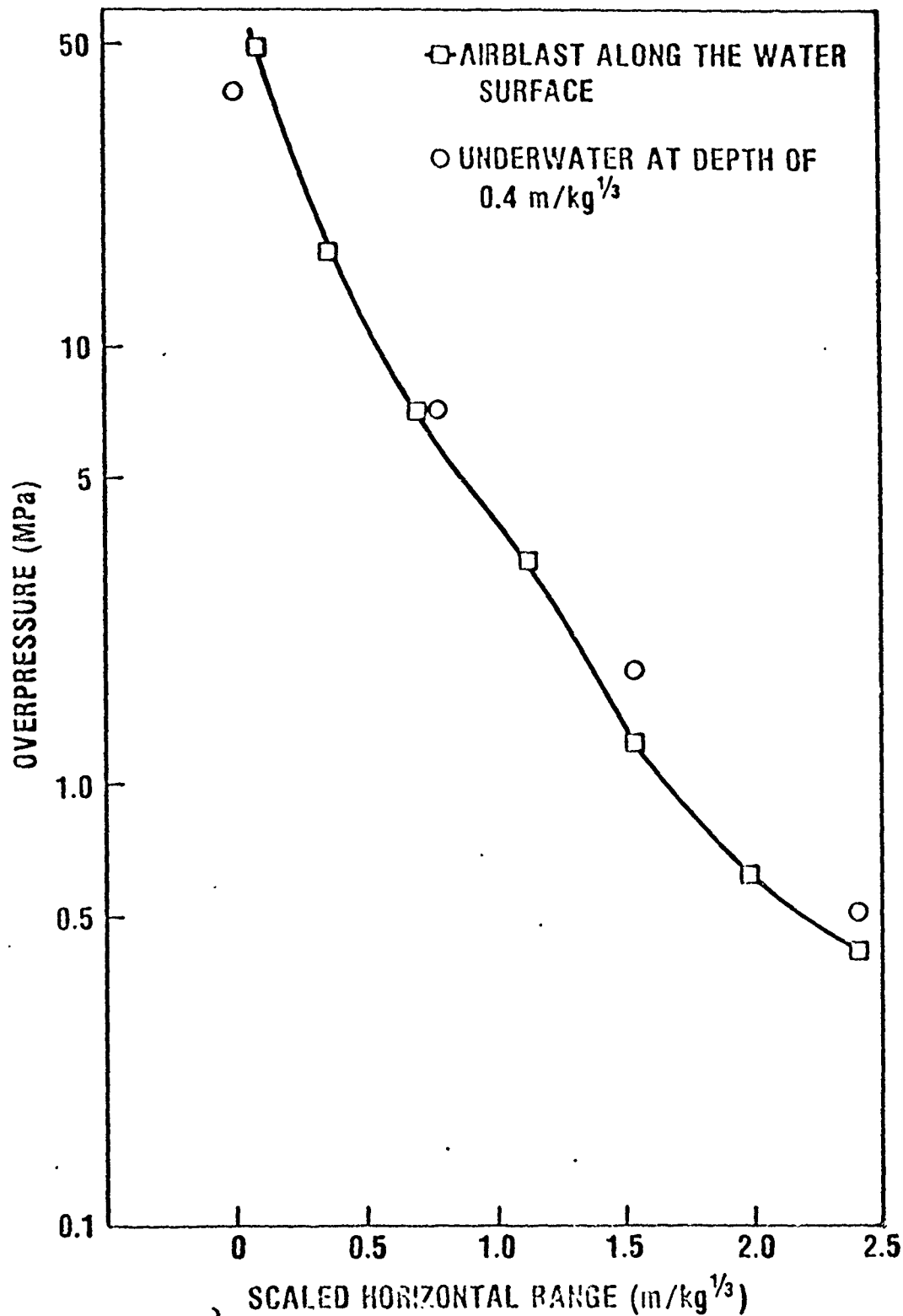


FIGURE 3.6



COMPARISON OF AIRBLAST AND UNDERWATER PRESSURES; PENTOLITE CYLINDERS FIRED AT HOB=1.0 m/kg<sup>1/3</sup>

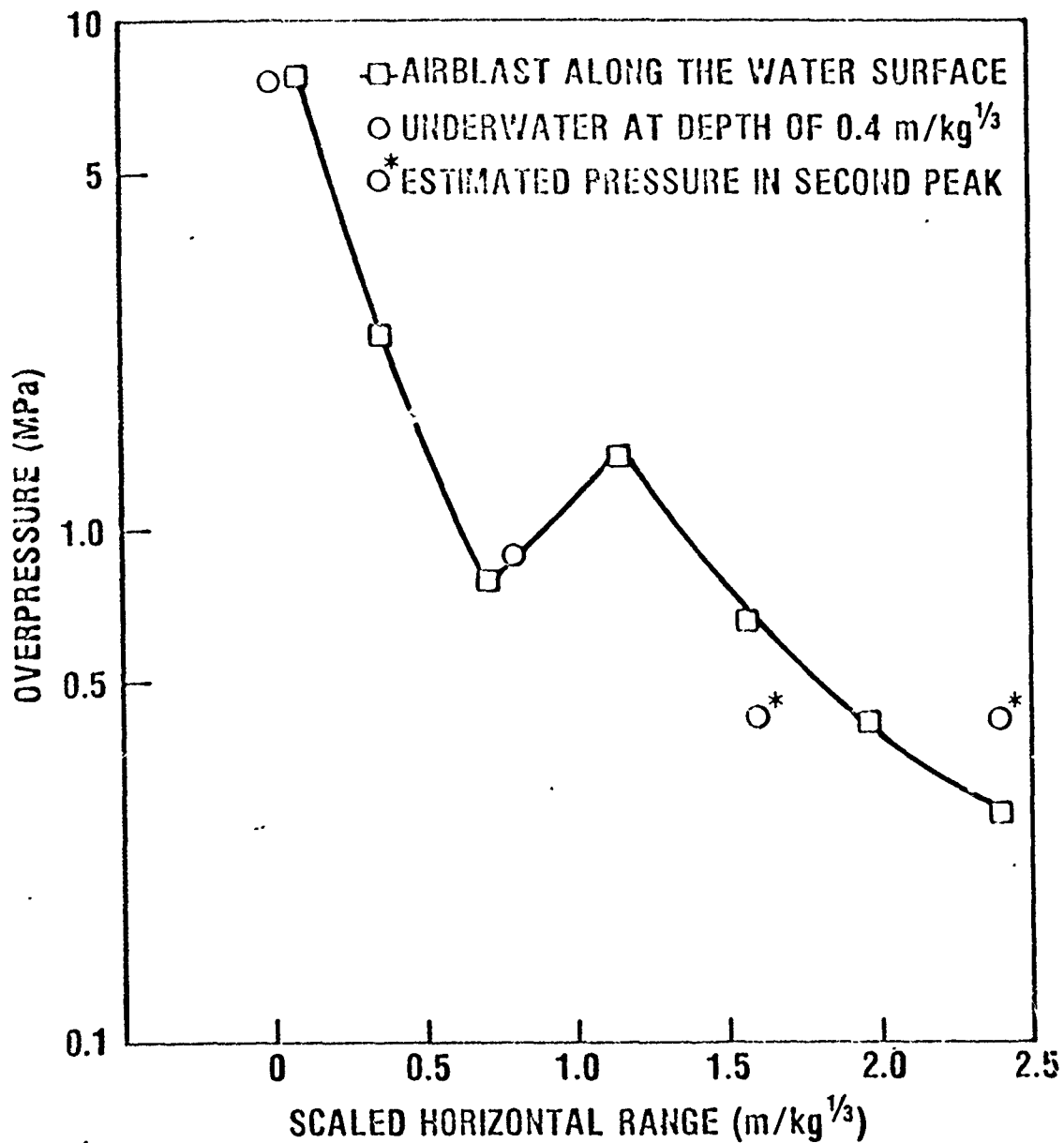


FIGURE 3.7



COMPARISON OF AIRBLAST AND UNDERWATER PRESSURES;  
PENTOLITE CYLINDERS FIRED AT  $\text{MOB}=1.6 \text{ m/kg}^{1/3}$

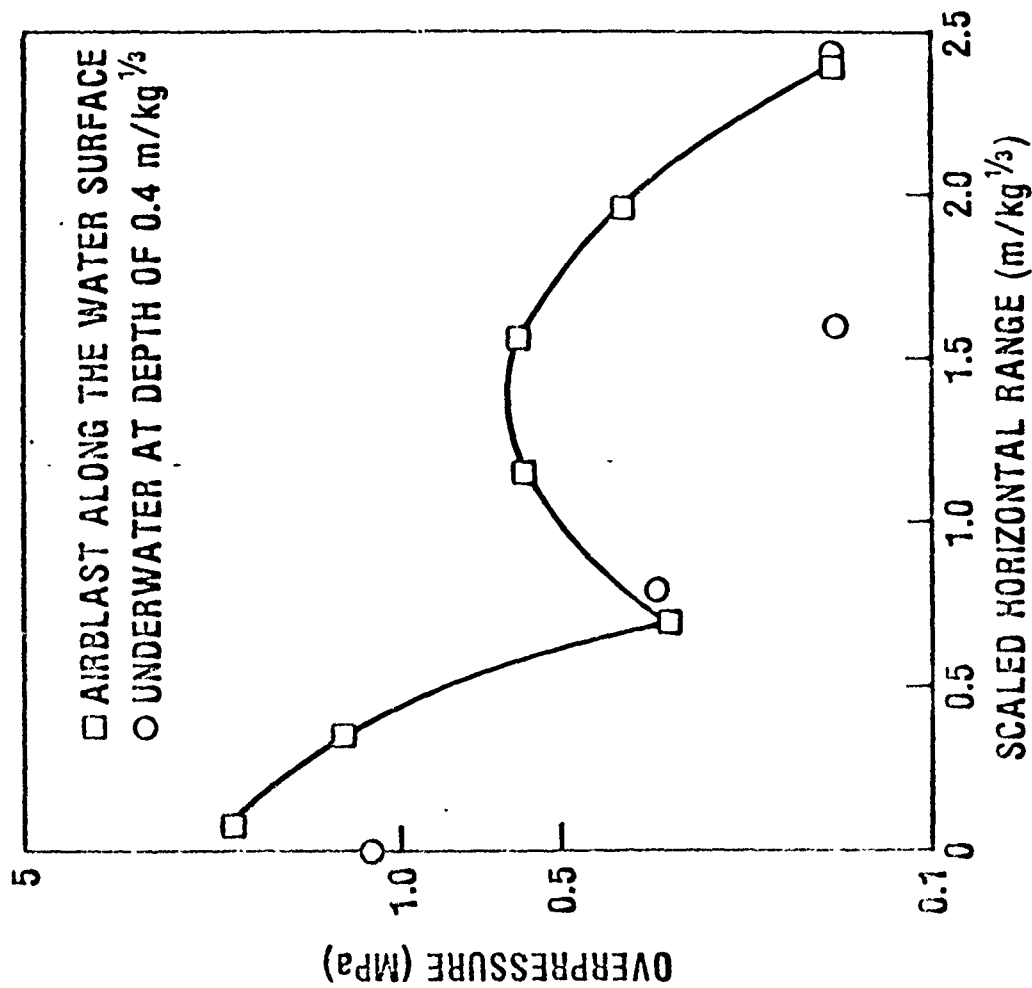
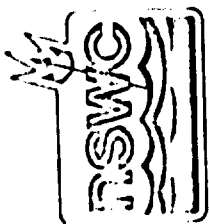


FIGURE 3.8



PENCILITE SPHERE CENTRALLY INITIATED,

$$HOB = 0.4 \text{ m/kg}^{1/3}$$

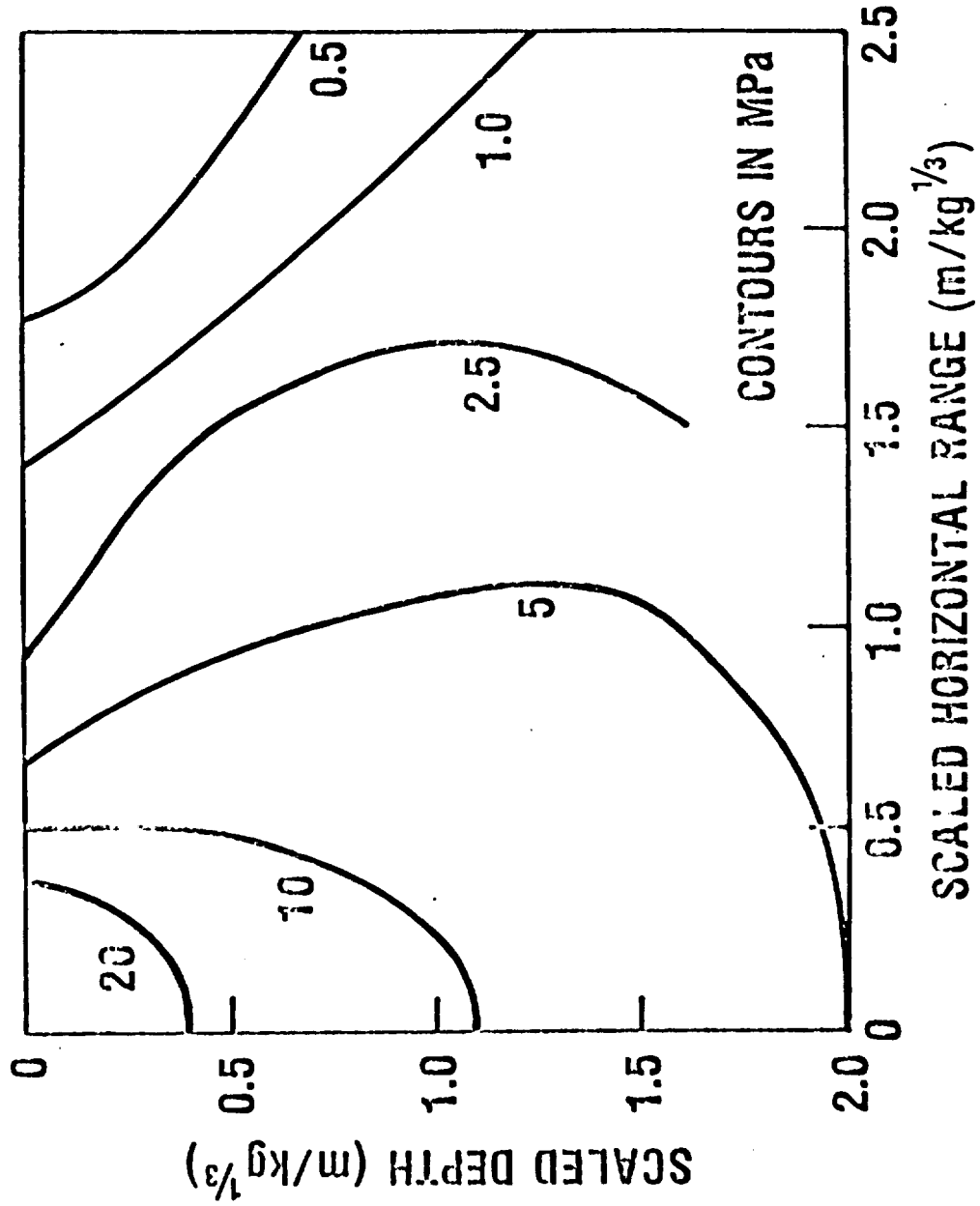
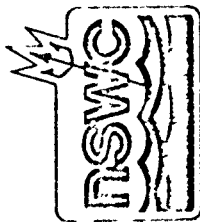


FIGURE 3.9



PENTOLITE SPHERE  $\text{HOB} = 1.6 \text{ m/kg}^{1/3}$

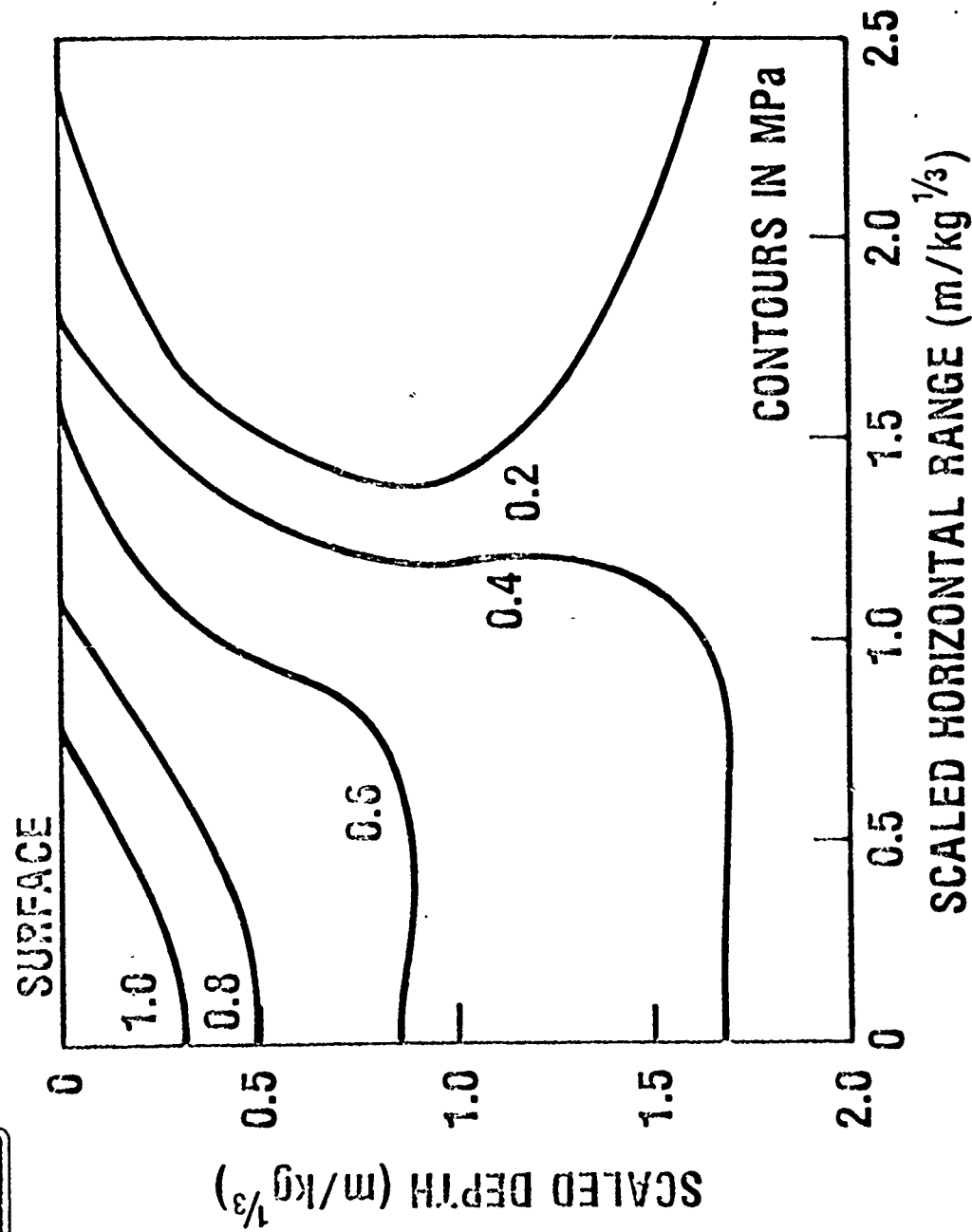


FIGURE 3.10



PENTOLITE CYLINDER CENTRALLY INITIATED,  
HOB = 0.4 m/kg<sup>1/3</sup>

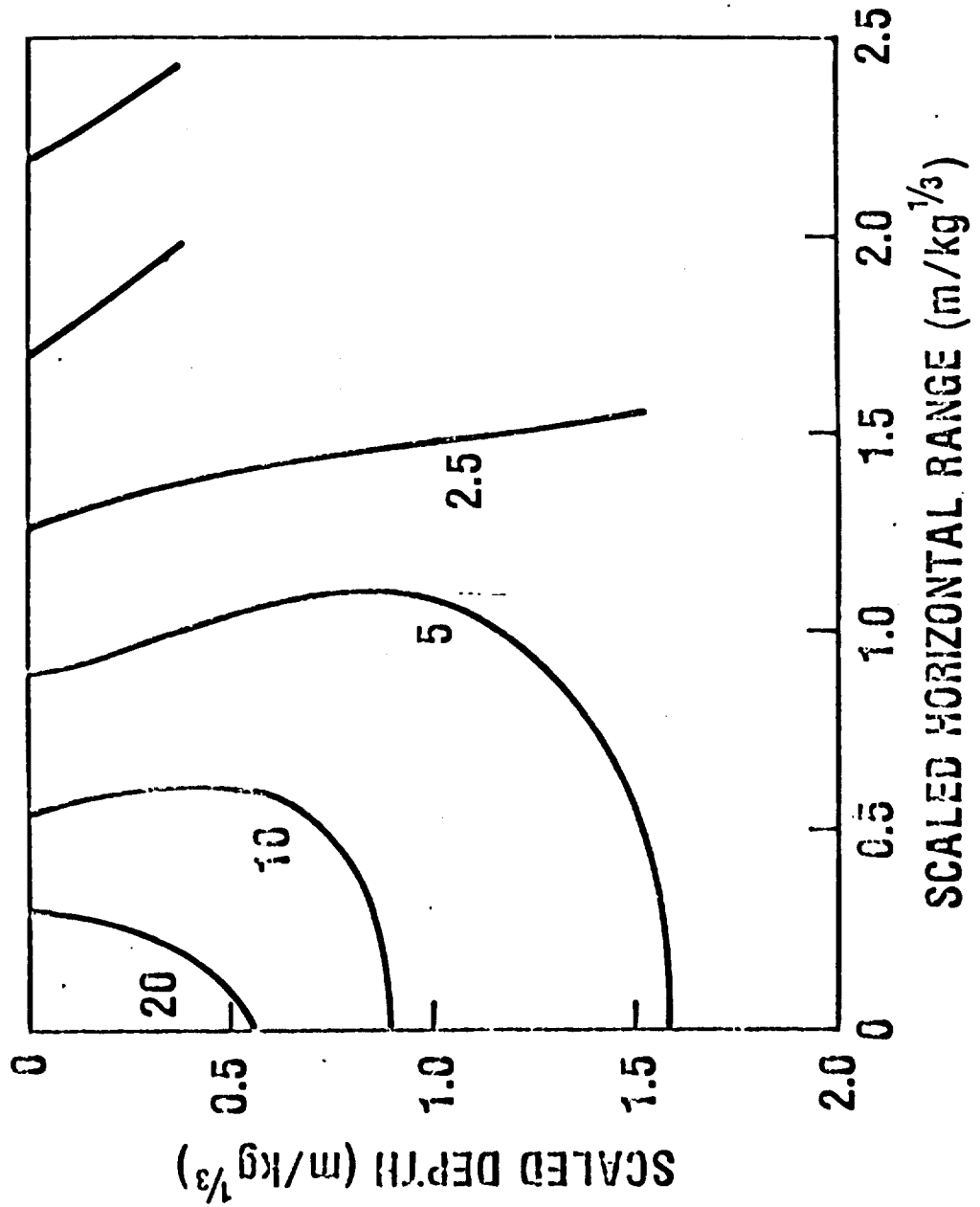
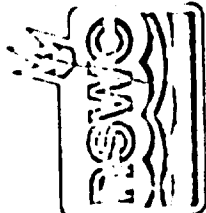


FIGURE 3.11



# PENTOLITE CYLINDER CENTRALLY INITIATED

HOB =  $1.6 \text{ m/kg}^{1/3}$

